Ernst Schering Foundation Symposium Proceedings, Vol. 4, pp. 125–152
DOI 10.1007/2789_2008_092

Published Online: 16 July 2008

Molecular Imaging of Tumor Metabolism and Apoptosis

U. Haberkorn(✉), A. Altmann, W. Mier, M. Eisenhut

Department of Nuclear Medicine, University of Heidelberg, INF 400, 69120 Heidelberg, Germany
email: *uwe.haberkorn@med.uni-heidelberg.de*

Abstract. Increased metabolism has been found to be one of the most prominent features of malignant tumors. This property led to the development of tracers for the assessment of glucose metabolism and amino acid transport and their application for tumor diagnosis and staging. Prominent examples are fluorodeoxyglucose, methionine and tyrosine analogs, which have found broad clinical application. Since quantitative procedures are available, these techniques can also be used for therapy monitoring. Another approach may be based on the noninvasive detection of apoptosis with tracers for phosphatidyl-serine presentation and/or caspase activation as surrogate markers for therapeutic efficacy. Finally, the evaluation of hypoxia with nitroimidazoles may be a valuable tool for prognosis and therapy planning.

1 Glucose Metabolism

Malignant tumors are tissues metabolizing glucose to lactate to a high extent. This increased glycolytic activity correlates with a high amount of mitochondrial-bound hexokinase in the tumor cells. In quickly growing tumor cells, the hexokinase activity is greatly enhanced, and up to 80% of the molecules are bound to the outer mitochondrial membrane. Changes in the expression of glycolysis-associated genes during the malignant transformation have been reported by several groups (Shawver et al. 1987; Flier et al. 1987; Bos et al. 2002): especially the gene encoding the glucose transporter subtype 1 (GLUT1) is activated early after transformation of cells with oncogenes such as src, ras or fps. An increase in the mRNA of GLUT1 is observed as early as 4–6 h after induction of the p21 c-H-ras oncoprotein, while morphological changes occur after 72–76 h. Furthermore, the increase in GLUT1 mRNA after ras transfection was independent of the growth rate. In vivo overexpression of GLUT1 and GLUT3 was found in a series of different human and experimental tumors. The increase in GLUT1 transcription can be used for imaging or therapy by cloning a reporter gene or a therapeutic gene such as suicide genes downstream of the GLUT1 promoter/enhancer elements (Haberkorn et al. 2002, 2005). Examples are the herpes simplex virus thymidine kinase (HSVtk) gene or the sodium iodide symporter, where adeno associated virus or retroviral vectors have been used to transfect tumor cells and to measure the uptake of specific substrates or to treat animals with genetically modified tumors (Sieger et al. 2003, 2004). In these studies, reporter gene expression (green fluorescent protein, HSVtk or sodium iodide symporter) was specific for tumor cells or cells with expression of an activated ras oncogene (Fig. 1).

^{18}Fluordeoxyglucose (FDG) for PET studies of glucose metabolism was introduced as a consequence of autoradiographic and biochemical studies with glucose analogs in different tissues. Similar to glucose, 2-deoxyglucose (dGlc) and FDG are transported bidirectionally and are phosphorylated by the enzyme hexokinase. This is possible because the C-2 position, unlike the C-1, C-3 and C-6 positions, is uncritical for the binding to the hexokinase. In contrast to glucose-6-phosphate, FDG-6-phosphate and dGlc-6-phosphate are not further metabolized in significant amounts during the examination. dGlc-6-phosphate is not

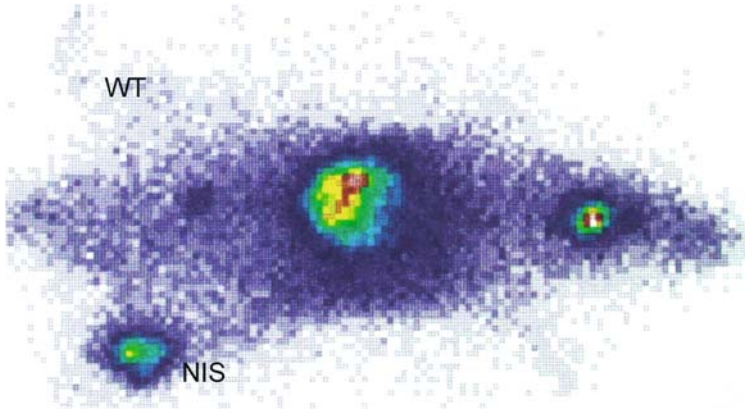

Fig. 1. Scintigraphic image of a rat bearing a wild type (*WT*) and a genetically modified tumor with expression of the human sodium iodide symporter (*NIS*). Only the NIS-expressing tumor, the stomach and the thyroid gland show accumulation of ^{131}I

metabolized to fructose-6-phosphate and, therefore, is not a substrate for the glucose-6-phosphate dehydrogenase. dGlc-6-phosphate may be converted to dGlc-1-phosphate and uridine-diphosphate(UDP)-dGlc, followed by an incorporation into glycogen, glycolipids and glycoproteins. However, these reactions are very slow in mammalian tissues. Furthermore, in the brain, the organ where the deoxyglucose method was applied for the first time, as well as in malignant tumors, glucose-6-phosphatase activity is downregulated. In contrast to the autoinhibition of the glucose phosphorylation, FDG-6-phosphate shows no inhibition of hexokinase activity. Compared to 2-deoxyglucose, FDG is incorporated very slowly into macromolecules, as has been demonstrated in yeasts as well as in chick fibroblasts. Due to their negative charge, which prevents penetration of the negatively charged inner part of the plasma membrane, FDG-6-phosphate and dGlc-6-phosphate accumulate in the cells. A further advantage is the rapid clearance of the tracer: similar to glucose, FDG shows glomerular filtration. However, unlike glucose, this is not followed by tubular reabsorption, because FDG is not a substrate for the tubular sodium glucose symporter, which is responsible for the rapid renal clearance.

PET studies with different animal models showed a correlation of FDG uptake and the content of GLUT1 and hexokinase mRNA (Haberkorn et al. 1994). Differences in the FDG uptake in different lung carcinomas, with lower values for adenocarcinomas as compared to squamous cell carcinomas, corresponded to the histologically determined expression of GLUT1, which was higher in squamous cell carcinomas than in adenocarcinomas. Therefore, the genetic program in malignant tumors leads to the corresponding FDG uptake values as measured with PET. Similar results were obtained in bronchioalveolar adenocarcinomas, with significantly lower values for the number of GLUT1-positive cells and FDG uptake and a correlation of histologic grade and the amount of GLUT1-positive cells and FDG uptake.

The clinical application of ^{18}FDG was predominantly for tumor diagnosis and staging for a variety of tumor entities such as lung, colon, breast, head and neck, and esophageal cancer, melanoma, and lymphoma (Fig. 2). In lung cancer, a meta-analytic comparison of PET (14 studies, 514 patients) and CT (29 studies, 2226 patients) for the demonstration of mediastinal nodal metastases in patients with non-small cell lung cancer (NLCLC) was done by Dwamena et al. (1999). In this analysis, pooled point estimates of diagnostic performance and summary ROC curves indicated that PET was significantly more accurate than CT for demonstration of nodal metastases with $p < 0.001$. The mean sensitivity and specificity were 0.79 ± 0.03 and 0.91 ± 0.02, respectively, for PET and 0.60 ± 0.02 and 0.77 ± 0.02, respectively, for CT. Subgroup analyses did not alter these findings. The results were collected and evaluated in a consensus conference leading to recommended applications of the method for a variety of tumors (Reske and Kotzerke 2001; Tables 1 and 2).

Besides staging, the prognostic value of FDG-PET has also been evaluated. The relation of high pretherapeutic FDG uptake to a poorer

Fig. 2. Transaxial PET/CT images of a patient with lung cancer. *Top:* CT image showing a large hilar mass. *Middle:* The fusion image demonstrates the smaller extent of the tumor and atelectatic lung tissue. *Bottom:* A metastasis in the adrenal gland is visualized

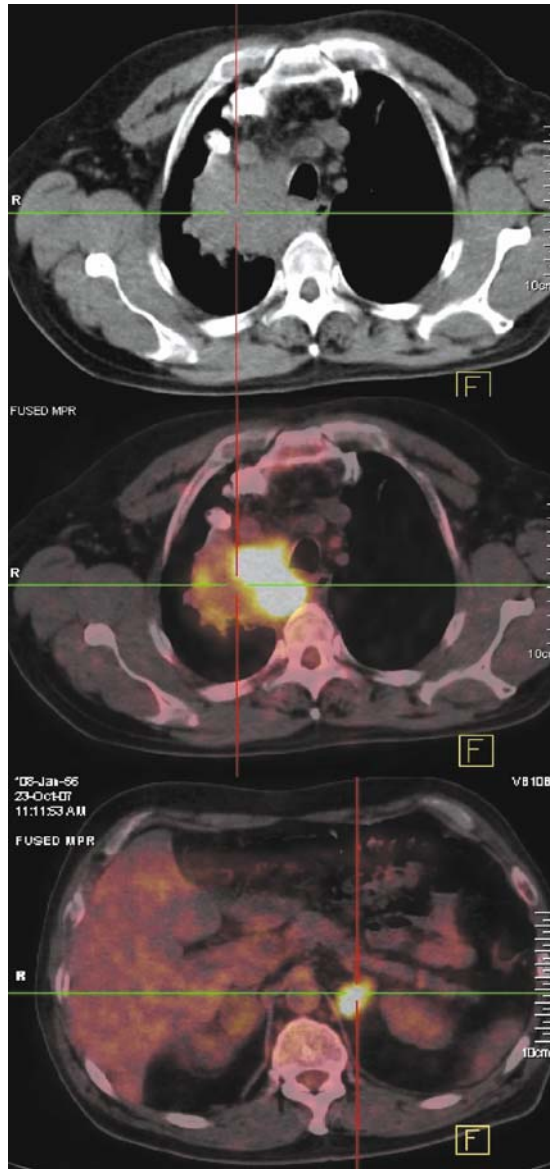
R
10cm
F
FUSED MPR
R
10cm
F
'08-Jan-66
23-Oct-07
11:11:53 AM
V8108
FUSED MPR
R
10cm
F

Table 1 Indications of FDG-PET with established or probable clinical value

Differentiated thyroid carcinoma	Restaging of radioiodine-negative lesions
	Restaging of radioiodine-positive lesions
Esophageal carcinoma	Staging lymph nodes, distant metastases
Pancreatic cancer	DD inflammation/tumor
	Recurrence
Colorectal carcinoma	Therapy monitoring
	Recurrence
Mammary carcinoma	N-staging
Head and neck tumors	N-staging
	Recurrence
	CUP
Lung tumors	Solitary pulmonary nodule
	N-staging (NSCLC)
	Extrathoracic N-staging
	Recurrence
Hodgkin lymphoma	Staging
	Therapy monitoring
Highly malignant NHL	Staging
	Therapy monitoring
Melanoma	N-staging (Breslow > 1.5 mm or known lymph node metastases)
	M-staging (Breslow > 1.5 mm or known lymph node metastases)
	Recurrence
	Follow-up for pT3 and pT4 tumors
	Follow-up of metastases
Bone/soft tissue tumors	Dignity, biological behavior, surgery planning

Table 2 Indications for a clinical value of FDG-PET in single cases

Mammary carcinoma	Dignity
	M-staging
Ovarian carcinoma	Recurrence
Head and neck tumors	Detection of a second tumor
Lung tumors	Therapy monitoring

prognosis was observed by different groups in patients with lung cancer (Ahuja et al. 1998; Vansteenkiste et al. 1999). In a study with 155 patients, the uptake in the primary lesion of NSCLC was compared to the clinical outcome: independent of other clinical findings, patients with higher uptake values had a shorter median survival time than patients with lower FDG accumulation (Ahuja et al. 1998). In this respect, a correlation was described between tumor growth and FDG uptake (Duhaylongsod et al. 1995). However, in experimental studies, conflicting reports exist concerning the possible correlation of FDG uptake and tumor cell proliferation (Brown et al. 1999; Higashi et al. 2000).

PET using ^{18}F-FDG has been applied for the evaluation of treatment response during chemotherapy, gene therapy, and radiotherapy in a variety of tumors, indicating that FDG delivers useful parameters for the early assessment of therapeutic efficacy (Bassa et al. 1996; Haberkorn et al. 1991, 1993, 1997a,b, 1998; Rozenthal et al. 1989). Furthermore, tumors may react to therapeutic intervention by compensatory reactions, including an increase in glucose metabolism, especially during the very early phase after treatment.

In general, increased FDG transport rates early after treatment are suggested as evidence of stress reactions in tumors after chemotherapy, gene therapy or radiation therapy (Haberkorn et al. 1998, 2001). The glucose carrier shows a complex regulation: glucose transport may be altered by phosphorylation of the transport protein (Hayes et al. 1993), decreased degradation (Shawver et al. 1987), translocation from intracellular pools to the plasma membrane (Widnell et al. 1990), or an increased expression of the gene (Flier et al. 1987). The increase in glucose transport after exposure of cells to damaging agents has been ascribed mainly to a redistribution of the glucose transport protein from intracellular pools to the plasma membrane. Such reactions have been found in cells exposed to arsenite, calcium ionophore A23187; or 2-mercaptoethanol (Widnell et al. 1990; Wertheimer et al. 1991; Hughes et al. 1989). Furthermore, increased glucose metabolism has been observed after chemotherapy or gene therapy of hepatoma with HSV thymidine kinase (Haberkorn et al. 1998, 2001a,b). Incubation with cytochalasin B or deoxyglucose after the end of treatment increased the amount of apoptotic cells (Haberkorn et al. 2001a,b), whereas monotherapy with these drugs had no effect. Enhanced glycolysis may be used

for a metabolic design of combination therapy, as has been done for chemotherapy (Haberkorn et al. 1992) or radiotherapy (Singh et al. 2005). These strategies intend to disturb possible repair processes that are in need of energy by interfering with glycolysis. Besides deoxyglucose, a few compounds are available such as 6-aminonicotinamide, 3-bromopyruvate, oxythiamine, 5-thioglucose, or genistein, where at least deoxyglucose shows a rather selective toxicity for cells with chemotherapy resistance (Haberkorn et al. 1992). The design of such a combination treatment requires data on the changes in the metabolic pathways with respect to dose and time dependence, which may be obtained by FDG-PET.

2 Amino Acids

Although PET with ^{18}F-fluorodeoxyglucose (FDG) has been proven to be useful for diagnosis and therapy monitoring in a variety of tumors, there is a need for complementary information of tumor biology. FDG is not tumor-selective and shows accumulation in inflammatory lesions. Furthermore, tissues with high background such as the brain may cause difficulties in image interpretation. Malignant tumors show changes in the amino acid transport, protein synthesis and proliferation. Therefore, many efforts have been made to establish tracers based on amino acids or proliferation markers.

Radiolabeled amino acids are used for measuring the rate of protein synthesis and amino acid transport. Besides protein synthesis, amino acids are precursors for many other biomolecules, such as adenine, cytosine, histamine, thyroxine, epinephrine, melanin and serotonin, and are important in other metabolic cycles, including transamination and transmethylation; methionine has a specific role in the initiation of protein synthesis and amino acids such as glutamine are used for energy. Since all these pathways create a dependency on amino acid uptake, amino acid transport does not faithfully represent protein synthesis, but rather provides a general measure of the cellular need for amino acids.

Amino acids enter cells mainly via specific transport systems (Christensen 1990). These systems can be sodium-dependent or -independent. Sodium-dependent transport relies on the sodium chemical gradient and

the electric potential across the plasma membrane, as well as on the activity of the Na^+/K^+-ATPase. Sodium-independent systems depend on the amino acid concentration gradient across the cell membrane and are often coupled to the countertransport (i.e., in the opposite direction) of K^+.

Kinetic studies have identified several sodium-dependent transport systems: A, ASC and Gly, which transport amino acids with short polar or linear side chains, e.g., alanine, serine and glycine. In general, a change in affinity occurs when a sodium ion binds to the transporter protein. Subsequent binding of the amino acid results in a conformational change in the transporter protein and in turn to the influx of the attached sodium ion and the amino acid into the cell. System A is transinhibited by intracellular substrates (i.e., the presence of intracellular substrates slows the uptake of amino acids), whereas system ASC is trans-stimulated by the presence of intracellular substrates (i.e., the presence of intracellular substrates increases the activity).

Sodium-independent systems, L (ubiquitously found), $B^{0,+}$ and y^+, are carriers for branched chain and aromatic amino acids, e.g., leucine, valine, tyrosine and phenylalanine. System L shows trans-stimulation by intracellular substrates such as leucine and valine. Most amino acid carrier systems can also transport synthetic, nonmetabolizable amino acid analogs.

Regulation of amino acid transport is complex and is influenced by hormones, cytokines, changes in cell volume and the availability of nutrients (Christensen 1990). For example, the number of system A active carriers increases during starvation; hence patients should be studied preferentially while fasting.

Malignant cells were found to have an increased amino acid transport (Boerner et al. 1985; Busch et al. 1959; Isselbacher 1972; Saier et al. 1988). Strong expression of system A has been found in transformed and malignant cells as a result of oncogene action (Saier et al. 1988) and a correlation between amino acid transport and cellular proliferation has been described (Jager et al. 2000; Kuwert et al. 1997).

For the assessment of the protein synthesis rate, relatively complex kinetic models are necessary. Furthermore, there is no existing constant correlation between the quantitative data derived from these models and the grade of malignancy (Ogawa et al. 1993). Although ^{11}C-leucine

appears to be the best amino acid for measuring protein synthesis rate (Vaalburg et al. 1992), most studies have used methionine because of the ease of tracer synthesis. The drawbacks of methionine are its use in metabolic cycles other than protein synthesis, which results in a variety of metabolites and difficulties in quantification (Ishiwata et al. 1989, 1996). Conflicting reports have been published about the specificity of carrier-mediated transport of methionine into brain tumors in studies comparing D- and L-methionine using an overload of branched amino acids. Furthermore, at least part of the tracer uptake seems to be the result of passive diffusion. Cellular uptake in vitro is mainly accomplished via the L system with minor contributions from systems A and ASC.

Patient studies have revealed high uptake of methionine in the pituitary gland and pancreas, moderate uptake in salivary glands, lacrimal glands and bone marrow, and low uptake in the normal brain (Jager et al. 2001). It has been used as a tracer mainly in brain tumors, where it shows excellent contrast between normal brain and tumors and high sensitivity for tumor detection (Herholz et al. 1998; Langen et al. 1997). Also, in a study of 196 patients, the accuracy of differentiation between low- and high-grade lesions was 79% (Herholz et al. 1998). Tumor delineation was better than with CT, MRI and FDG-PET (Mosskin et al. 1986; Bergstrom et al. 1983; Kaschten et al. 1998).

A high sensitivity for the detection of primary and metastatic brain tumors was also found using either ^{11}C-tyrosine or L-2-^{18}F-fluorotyrosine (Wienhard et al. 1991; Willemsen et al. 1995). Analysis of the plasma metabolites of ^{11}C-tyrosine revealed that ^{11}C-CO_2, ^{11}C-proteins and ^{11}C-L-DOPA constituted more than 50% of total plasma radioactivity at 40 min after injection making a complex pharmacokinetic model for further analysis necessary. Using a five-compartment model, it was shown that while the net protein synthesis rate was dependent on the recycling of amino acids from protein, tracer influx into the cell was not. The curve-fitting results of dynamic scans were unreliable because of the exchange of ^{11}C-tyrosine between plasma and erythrocytes, whereas the graphical Patlak-Gjedde analysis was not influenced by this. L-2-^{18}F-fluorotyrosine was studied in 15 patients with brain tumors and showed rapid uptake, which was mainly attributed to an increase in transport. Also, an improved localization of tumor tissue for biopsy has been described for both methionine and tyrosine.

In head and neck cancer, amino acids have been used mainly for staging. Primary tumors have shown higher methionine uptake as compared to surrounding tissues, and tumors larger than 1 cm in diameter have been detected with a sensitivity of 91% (Leskinen-Kallio et al. 1994). Noninvasive tumor grading has not been possible (Lindholm et al. 1998). Tyrosine-PET has shown comparable results with a significantly higher protein synthesis rate for tumor as compared to nontumor tissue (deBoer et al. 2002).

Lung cancer has also shown high uptake of methionine with high sensitivity, but low specificity, for solitary pulmonary nodules (Kubota et al. 1990). Staging was improved by methionine in a retrospective study, but gave no advantage as compared to FDG-PET.

Comparisons of FDG and amino acids in patients with breast cancer have revealed that FDG was better than tyrosine, but not as good as methionine (Jansson et al. 1995). In lymphoma, no association between methionine uptake with histologic grade has been seen, unless kinetic analysis was applied (Rodriguez et al. 1995). Differentiation between benign and malignant lesions has also been possible for soft tissue sarcomas using tyrosine-PET (Plaat et al. 1999). Studies with small patient numbers have been conducted either with methionine or tyrosine in patients with melanoma, bladder cancer, metastatic nonseminoma, ovarian cancer and uterine cancer.

Since ^{123}I-α-methyl tyrosine (^{123}I-IMT) has proven to be a promising SPECT tracer for imaging amino acid transport in tumors (Fig. 3), ^{124}I-IMT and L-3-^{18}F-α-methyl tyrosine (FMT) have been synthesized for PET studies (Amano et al. 1998; Langen et al. 1990). ^{124}I-IMT accumulates in brain and tumor tissue, reaching a maximum concentration after 15 min with a washout of 20%–35% at 60 min after injection. Animal experiments have confirmed the accumulation of the intact tracer in brain without incorporation of the tracer into proteins. FMT uptake was high in the pancreas and in several tumor models. Tumor uptake of FMT was reduced by inhibition of the amino acid transport systems. The tumor:blood ratios of FMT in mice with LS180 (human colon cancer), RPMI1788 (human B-cell lymphoma) and MCF7 (human mammary carcinoma) tumors at 60 min after injection were 1.8, 5.9 and 3.6, respectively. Most of the activity was localized in the acid-soluble fraction, suggesting that FMT is mainly not incorporated into proteins.

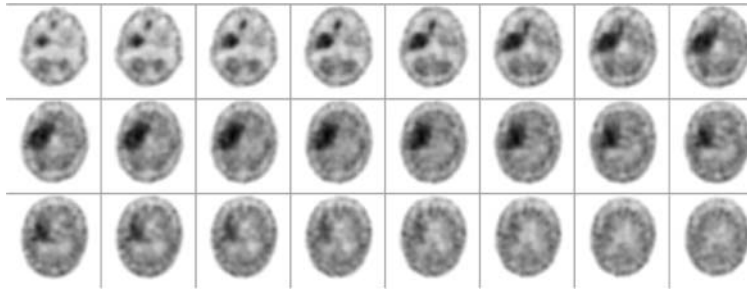

Fig. 3. Transaxial PET/CT images of a patient with lung cancer. *Top:* CT image showing a large hilar mass. *Middle:* The fusion image demonstrates the smaller extent of the tumor and atelectatic lung tissue. *Bottom:* A metastasis in the adrenal gland is visualized

Clinical studies have shown that brain tumors are better delineated by FMT as compared with FDG, with no dependence of FMT uptake on tumor grade (Inoue et al. 1999). In contrast, FMT uptake correlated with histologic grade in musculoskeletal tumors, but with a better discriminative capacity for FDG.

O-(2-^{18}F-fluoroethyl)- L-tyrosine (L-FET), which is also not incorporated into proteins, has been evaluated in mammary carcinoma-bearing mice and in mice with the colon carcinoma cell line SW707 (Wester et al. 1999; Heiss et al. 1999). Results of transport inhibition experiments with specific competitive inhibitors have demonstrated that the uptake of L-FET into SW707 cells is caused mainly by system L. In vivo studies revealed a plasma half-life of L-FET of 94 min and increasing brain uptake up to 120 min with a brain:blood ratio of 0.9. Xenotransplanted tumors have shown higher uptake of L-FET (> 6% injected dose/g) than all other organs, except the pancreas. High-performance liquid chromatography (HPLC) analysis of brain, pancreas and tumor homogenates as well as plasma samples of mice at 10, 40 or 60 min after injection revealed only unchanged L-FET, indicating high stability and lack of metabolization of the tracer. Preliminary clinical results are available for high-grade brain tumors and metastatic melanomas (Weber et al. 2001).

Once transported into the cell, tyrosine is metabolized to dihydroxyphenylalanine (DOPA), which can be used for melanin synthesis. Therefore, DOPA labeled with ^{18}F at the 2 position has been used for tumor characterization in melanoma-bearing mice (Ishiwata et al. 1991). Tumors with a lower melanin synthesis rate accumulated less DOPA than tumors with a higher rate. The metabolite predominantly found in these studies was ^{18}F-MeFDOPA. DOPA labeled at the 6 position is commonly used for the evaluation of the dopaminergic system. It has also been used to study patients with metastatic melanoma; tracer uptake was perfusion-independent with DOPA-PET showing a lower sensitivity as compared to FDG-PET (Dimitrakopoulou-Strauss et al. 2001).

A variety of synthetic amino acids, including α-aminoisobutyric acid (AIB), 1-aminocyclopentane carboxylic (ACPC) acid, 2-amino-3-fluoro-2-methylpropanoic acid (FAMP), 3-fluoro-2-methyl-2-(methylamino)propanoic acid (N-MeFAMP) and 1-amino-3-fluorocyclobutane-1-carboxylic acid (FACBC), have been synthesized and evaluated, mostly in cell culture and animal systems. AIB is thought to be actively accumulated in viable cells primarily by the A-type amino acid transport system and has shown avid uptake in a melanoma model. Additionally, ACPC and AIB imaging were found to be superior to FDG in C6 gliomas and Walker 256 rat carcinosarcoma, especially for identifying tumor infiltration of adjacent brain tissue beyond the macroscopic border of the tumor, and in low-grade tumors with an intact blood–brain barrier. Contrast-enhancing regions of the tumors were visualized more clearly with AIB than with FDG or Ga-DTPA; viable and necrotic-appearing tumor regions could be distinguished more readily with AIB than with FDG (Uehara et al. 1997). Increased AIB uptake was also observed in soft tissue sarcomas (Schwarzbach et al. 1999). As for AIB, amino acid transport assays using 9L gliosarcoma cells demonstrated that FAMP and N-MeFAMP are substrates for the A type amino acid transport system and show very high tumor:normal brain ratios: 36:1 and 104:1, respectively (McConathy et al. 2002). In a rat brain tumor model, maximum tumor uptake of ^{18}F-FACBC was seen at 60 min, with a tumor:normal brain ratio of 5.6 at 5 min and 6.6 at 60 min after tracer administration (Shoup et al. 1999).

Measurement of the effects of therapy on tumor metabolism may be useful in predicting therapy outcome at an early stage of treatment. This principle may be applied not only to glucose metabolism but also to amino acid transport and metabolism. Studies of different human tumors treated with a variety of therapies and of the rat AH109A tumor model after radiotherapy demonstrated a rapid posttherapeutic reduction in methionine uptake, reflecting inactivation of protein synthesis and damage to the membrane transport system (Jansson et al. 1995; Bergstrom et al. 1987; Schaider et al. 1996). Furthermore, the uptake of L-1-^{11}C-tyrosine in rhabdomyosarcoma of Wag/Rij rats was dose-dependently reduced after local hyperthermia (Daemen et al. 1991). Moreover, the accumulation of AIB is decreased in rat prostate tumors after long-term treatment with stilbestrol (Dunzendorfer et al. 1981). These changes were followed later by a reduction in tumor mass.

In vitro studies have demonstrated that methotrexate and cisplatin induce a *decline* in AIB and methionine accumulation in L1210 murine leukemia cells (Scanlon et al. 1983, 1987), leading to the speculation that the inhibition of methionine uptake by methotrexate may be due to drug binding to a specific membrane carrier, or a reduction in the sodium gradient across the plasma membrane, which is necessary for the uptake of amino acids, or effects on intracellular processes which support uptake of amino acids. Higashi et al. demonstrated an *increase* in methionine and FDG uptake in human ovarian carcinoma cells after radiotherapy, which was accompanied by an increase in cell volume (Higashi et al. 1993). These phenomena were interpreted as giant cell formation with enlarged cellular volume and continued protein synthesis, but accelerated repair was also suggested. Another in vitro study combined the information obtained from experiments using a transport tracer (AIB) and a tracer that is transported and metabolized (methionine) and found a decrease in neutral amino acid transport after gene therapy of hepatoma cells with HSV thymidine kinase and ganciclovir, indicating treatment effects on the energy-dependent transport systems (Haberkorn et al. 1997a). Methionine uptake experiments showed a decrease in tracer accumulation in the acid-insoluble fraction (representing nucleic acids and proteins), indicating impaired protein synthesis and an increase in the acid-soluble fraction. The increase in radioactivity in the acid-soluble fraction may be caused by enhanced transmethy-

lation processes, which usually are observed during oncogenic transformation and after exposure to DNA-damaging agents.

Clinical studies in brain tumors have been done for early evaluation of treatment response and differentiation between recurrence and radiation necrosis. In ten patients with low-grade gliomas, a dose-dependent reduction in methionine uptake was seen after brachytherapy (Wurker et al. 1996). Differentiation between radiation necrosis and tumor recurrence was possible with methionine-PET (Ogawa et al. 1991). In another study with ten patients, tyrosine-PET showed no change in the protein synthesis rate despite a decrease in tumor volume in seven patients (Heesters et al. 1998).

After radiotherapy of head and neck cancer, a lower posttherapeutic methionine uptake was shown to correlate with therapy response (Lindholm et al. 1998). Similar results were obtained in patients after radiotherapy or chemotherapy of lung, breast and rectal cancer (Jansson et al. 1995; Daemen et al. 1991). However, the predictive value of methionine-PET remains questionable.

Amino acids have been suggested to be useful in the differentiation between inflammation and malignancy. Experimental studies have shown that amino acids accumulate less than FDG in inflammation (Kubota et al. 1989). However, uptake may occur in benign lesions such as ischemic brain, infarction, scar, abscesses and sarcoidosis, and also in irradiated areas. Therefore, active inflammatory cells may need amino acids and the specificity of amino acids for tumor imaging is not absolute. However, in mice with tumor-infiltrated or inflammatory lymph nodes, the accumulation of *O*-(2-^{18}F-fluoroethyl)-L-tyrosine showed significant differences with no overlap between inflammatory and tumorous nodes (Rau et al. 2002).

In summary, amino acids may have a potential role in the characterization of the biological properties of tumors as increased amino acid transport or protein synthesis. Advantages over FDG imaging can be expected in the imaging of brain tumors, because the background of tracer accumulation is lower than FDG. The role of amino acids for the monitoring of tumor response to treatment as well as the differentiation between inflammation and tumor tissue has to be established in further studies.

3 Apoptosis

For the in vivo detection of apoptosis, two main targets in the apoptotic pathway are of interest: (1) the presentation of phosphatidylserine residues at the outer side of the plasma membrane and (2) the appearance of activated caspases (Martin et al. 1995; Villa et al. 1997). Phosphatidylserine is maintained at the inner site of the plasma membrane by the adenosine triphosphate (ATP)-dependent enzymes floppase and translocase (Zwaal and Schroit 1997). Apoptosis induced inactivation of these enzymes and activation of a scramblase leads to the appearance of phosphatidylserine on the outer side of the membrane. This effect has been recently used to develop an imaging agent for apoptosis (Blankenberg et al 1998, 1999): Annexin V, a 35-kDa human protein with high affinity for cell membrane-bound phosphatidylserine, was labeled with ^{99m}Tc and investigated for its uptake in apoptotic cells. An increased accumulation was found in Jurkat cells where the programmed cell death was initiated by growth factor deprivation, anti-CD95 antibody and doxorubicin treatment. Also, anti-CD95 treated mice showed a threefold rise in hepatic ^{99m}Tc-Annexin V accumulation in response to severe liver damage with histologic evidence of apoptosis. Finally, increased uptake was detected in animal models using the acute rejection of transplanted heterotopic cardiac allografts or transplanted murine B cell lymphomas treated with cyclophosphamide (Blankenberg et al. 1999).

Since caspases play a key role during the early period of the intracellular signal cascade of cells undergoing apoptosis, benzyloxycarbonyl-Val-Ala-DL-Asp(*O*-methyl)-fluoromethyl ketone [Z-VAD-fmk], a pancaspase inhibitor, was evaluated as a potential apoptosis imaging agent (Haberkorn et al. 2001c). Uptake measurements were made with Morris hepatoma cells (MH3924Atk8), which showed expression of the herpes simplex virus thymidine kinase (HSVtk) gene. Apoptosis was induced by treatment of the cells with ganciclovir and a twofold increase of [^{131}I]I-Z-VAD-fmk uptake was found at the end of treatment with the HSVtk/suicide system, which consistently remained elevated for the following 4 h. The slow cellular influx and lack of uptake saturation of [^{131}I]IZ-VAD-fmk are evidence for simple diffusion as a transport mechanism. In addition, the absolute cellular uptake of [^{131}I]IZ-VAD-fmk was found to be low. Instead of using an inhibitor, synthetic

caspase substrates that may accumulate in the apoptotic cell by metabolic trapping, thereby enhancing the imaging signal are currently being investigated. In a recent study, ten radiolabeled peptides containing the DEVDG sequence, selective for downstream caspases such as caspase-3, were synthesized and evaluated for their uptake kinetics using an apoptosis test system (Bauer et al. 2005). Within this series of peptides, radioiodinated Tat49–57-yDEVDG-NH2 and Tat57–49-yDEVDG-NH2, both containing an additional HIV Tat sequence, were taken up by apoptotic cells to a significantly higher extent than with the controls. The enhanced uptake was interpreted as the interaction of the labeled peptide or fragment with activated caspases. Current efforts are focused on alternative radioisotopes that include radiometal complexes to further improve these characteristics.

4 Hypoxia

Because of uncontrolled growth and a misbalance between tumor mass and vascularization, oxygen limitation is a common feature of malignant tumors. Oxygen concentration inside solid tumors is reduced, which contributes to the tumor aggressiveness and poor prognosis of patients (Stadler et al. 1999). Genomes of tumor cells become unstable under hypoxic conditions, and hypoxia can be the selective pressure for the expansion of clones with anti-apoptotic treatment-resistant or highly metastatic potential (Young et al. 1988; Graeber et al. 1996). Resistance to chemotherapy and radiation therapy can be attributed, at least in part, to the hypoxic condition of tumor cells (Teicher 2004). Hypoxia confers these aggressive properties on the tumors through either the remodeling of tumor vasculature or the direct phenotypic changes of tumor cells themselves. Tumor cells under hypoxia can acquire anti-apoptotic and chemoresistant properties through changes in the expression of apoptosis-related molecules. Furthermore, the involvement of HIF-1α in the tumor progression to an anti-apoptotic phenotype was reported (Erler et al. 2004).

Oxygen deprivation is encountered by the induction of various genes. Hypoxia inducible factor 1 (HIF) plays a central role in this regulatory system. HIF can induce the production of a variety of gene products

relevant for metabolism, vascularization, survival, pH and cell migration. Active HIF-1 is a heterodimer composed of two subunits, HIF-1α and HIF-1β. HIF-1β is constitutively expressed independent of environmental oxygen concentration, while the expression of HIF-1α is negligible under normoxia and induced under hypoxia. Up to now, HIF-1α, HIF-2α and HIF-3α have been identified and cloned as the members of HIF α family that can dimerize with HIF-1α and bind to hypoxia responsible elements (HRE) in the genes of hypoxia-responsive molecules.

Among HIFα family members, HIF-1α is thought to be the key molecule regulating the cellular response to physiological and pathological hypoxia. Mechanisms of hypoxia-induced expression of HIF-1α have been intensively studied, and the intracellular level of HIF-1α protein under reduced oxygen concentration was found to be increased mainly through stabilization of the protein. Turnover of the HIF-1α protein is regulated by the ubiquitin–proteasome system, in which target proteins are degraded by proteasome depending on their ubiquitylation (Semenza 2002). Under normoxia, the level of the HIF-1α protein is kept low through rapid ubiquitylation and subsequent proteasomal degradation. HIF-1α becomes susceptible to rapid ubiquitylation through hydroxylation of proline residues at Pro-402 and Pro-564 by prolyl hydroxylase 2 (PHD2), which requires oxygen for its enzyme activity (Berra et al. 2003). In cells under hypoxia, the ubiquitylation and subsequent degradation of HIF-1α is suppressed because of the decrease in PHD2 activity, and therefore the level of HIF-1a protein increases. In addition, the activity of HIF-1 as a transcription factor is also controlled by hydroxylation of HIF-1α protein. Hydroxylation of asparagine residue at Asn-803 inhibits the interaction between HIF-1α and p300, which is essential for the transcriptional activity of HIF-1 (Lando et al. 2002b). Because the factor inhibiting HIF (FIH) that hydroxylates Asn-803 is also an oxygen-dependent enzyme, the transcriptional activity of HIF-1 increases under hypoxia due to the suppressed hydroxylation at Asn-803 (Lando et al. 2002a; Hewitson et al. 2002). Cells can control the transcription of HIF-1-regulated genes by sensing the oxygen concentration through the activities of oxygen-dependent enzymes PHD2 and FIH, and consequently regulating the intracellular level as well as the transcriptional activity of HIF-1 (Haddad 2002).

Although HIF-1 can be activated by nonhypoxic pathways, hypoxia inside the growing tumor mass is the most probable candidate for the activation of HIF-1α cascade in tumor cells. This is supported by the fact that both HIF-1α and VEGF expression are upregulated predominantly in tumor cells around the necrotic areas of highly vascularized tumor mass in glioblastoma (Plate et al. 1992). Therefore, angiogenesis triggered by the hypoxia-HIF-1α-VEGF cascade seems to play an important role in tumor progression to the more aggressive phenotypes.

The noninvasive imaging of hypoxic areas may be used for the development of individualized therapies, new therapeutic approaches or as a prognostic marker. At present, oxygen partial pressure (pO_2) is measured with the Eppendorf probe, which showed significant correlations of pO_2 and therapy response in clinical studies. This method has several limitations: its application is restricted to lesions located at surface areas and its invasiveness precludes it from being done routinely or repeatedly. Furthermore, differentiating between areas of necrosis and areas with anoxic/hypoxic but living cells is not possible.

Nitroimidazoles are reduced under hypoxic conditions by intracellular reductases to reactive intermediate metabolites. This process is dependent on the hypoxia level and may lead up to a 40-fold increase in the amount of reduced products. The metabolites bind covalently to thiol moieties of intracellular proteins, leading to an accumulation in living hypoxic cells. The resulting complexes can then be detected with antibodies, MRS, flow cytometry, autoradiography and scintigraphy or PET. 2-nitroimidazole can be labeled with ^{18}F, ^{123}I, ^{131}I (iodinated azomycinarabinoside, IAZA) and ^{99m}Tc. In vitro studies and animal experiments showed the selectivity of [^{18}F]Fluoromisonidazole for hypoxic cells. Tracer accumulation was quantitated with mathematical models as well as by determining the SUV. The results obtained so far show that [^{18}F]FMISO uptake measurements underestimate the amount of hypoxia at very low pO_2-values (2–3 mmHg). This is probably caused by the fact that below a defined cutoff level the reduction processes can no longer be increased.

Clinically, [^{18}F]FMISO was applied for the assessment of myocardial ischemia, tumor hypoxia in head and neck tumors, gliomas, non-small cell lung tumors and in soft tissue sarcomas (Padhani et al. 2007; Lee and Scott 2007). Quantitation was done by determining the hypoxic

fraction volume (FHV), which is defined as the procentual fraction of tumor pixels showing a tracer accumulation at 2 h after infection at least 1.4-fold higher than the activity in plasma. After radiation therapy, a significant decrease of the FHV has been observed. However, the tracer uptake was not dependent on the tumor size, grading or VEGF expression. In patients with non-small cell lung cancer or head and neck cancer, 97% of the tumors showed accumulation of the tracer, with a great variability in the extent in different tumor entities, however, but also in different lesions from the same patient.

4-[^{18}F]Fluoro-2,3-dihydroxy-1–2(2′-nitro-1′-imidazolyl)butane([^{18}F]Fluoroerythroimidazol, [^{18}F]FETNIM) showed higher tumor:blood and tumor:muscle ratios in animal experiments than [^{18}F]FMISO (Grönros et al. 2004). The tracer accumulates strongly in liver and tumor, with no binding to plasma proteins and no peripheral metabolization. In patients with head and neck tumors, better tumor:muscle ratios were obtained in comparison to [^{18}F]FMISO.

Preliminary results have been reported for the evaluation of ^{62}Cu-labeled diacetyl-bis(N4-methylthiosemicarbazone) (^{62}Cu-ATSM) as a possible hypoxia imaging agent (Padhani et al. 2007). ^{62}Cu-ATSM showed a rapid clearance from the blood in all patients, with a low uptake in lung tissue and an intense accumulation in tumors. Furthermore, a negative correlation was found between blood flow and the flow-normalized ^{62}Cu-ATSM uptake in three out of four patients. This was interpreted as evidence for an increased ^{62}Cu-ATSM accumulation under conditions of low blood flow.

In summary, all these imaging procedures may be used to characterize the biological features of tumors and their metastases with respect to metabolism, apoptosis and microenvironment. The information obtained with these techniques can be expected to individualize treatment and make radioisotope-based methods promising tools for tumor detection, therapy planning, and therapy monitoring.

References

Ahuja V, Coleman RE, Herndon J, Patz EF (1998) Prognostic significance of FDG-PET imaging in patients with non-small cell lung cancer. Cancer 83:918–924

Amano S, Inoue T, Tomiyoshi K et al (1998) In vivo comparison of PET and SPECT radiopharmaceuticals in detecting breast cancer. J Nucl Med 39:1424–1427

Bassa P, Kim EE, Inoue T, Wong FC, Korkmaz M, Yang DJ, Hicks KW, Buzdar AU, Podoloff DA (1996) Evaluation of preoperative chemotherapy using PET with fluorine-18-fluorodeoxyglucose in breast cancer. J Nucl Med 37:931–938

Bauer C, Bauder-Wuest U, Mier W, Haberkorn U, Eisenhut M (2005) ^{131}I-labeled peptides as caspase substrates for apoptosis imaging. J Nucl Med 46:1066–1074

Bergstrom M, Collins VP, Ehrin E et al (1983) Discrepancies in brain tumor extent as shown by computed tomography and positron emission tomography using [^{68}Ga]EDTA, [^{11}C]glucose, and [^{11}C]methionine. J Comput Assist Tomogr 7:1062–1066

Bergstrom M, Muhr C, Lundberg PO et al (1987) Rapid decrease in amino acid metabolism in prolactin-secreting pituitary adenomas after bromocriptine treatment: a PET study. J Comput Assist Tomogr 11:815–819

Berra E, Benizri E, Ginouves A, Volmat V, Roux D, Pouyssegur J (2003) HIF prolyl-hydroxylase 2 is the key oxygen sensor setting low steady-state levels of HIF-1alpha in normoxia. EMBO J 22:4082–4090

Blankenberg FG, Katsikis PD, Tait JF, Davis RE, Naumovski L, Ohtsuki K et al (1998) In vivo detection and imaging of phosphatidylserine expression during programmed cell death. Proc Natl Acad Sci U S A 95:6349–6354

Blankenberg FG, Katsikis PD, Tait JF, Davis RE, Naumovski L, Ohtsuki K et al (1999) Imaging of apoptosis (programmed cell death) with 99mTc annexin V. J Nucl Med 40:184–191

Boerner P, Saier MH (1985) Adaptive regulatory control of system A transport activity in a kidney epithelial cell line (MDCK) and in a transformed variant. J Cell Physiol 122:308–315

Bos R, van Der Hoeven JJ, van Der Wall E, van der Groep P, van Diest PJ, Comans EFI, Joshi U, Semenza GL, Hoekstra OS, Lammertsma AA, Molthoff CFM (2002) Biologic correlates of (18)fluorodeoxyglucose uptake in human breast cancer measured by positron emission tomography. J Clin Oncol 20:379–387

Brown RS, Leung JY, Kison PV, Zasadny KR, Flint A, Wahl RL (1999) Glucose transporters and FDG uptake in untreated primary human non-small cell lung cancer. J Nucl Med 40:556–565

Busch H, Davis JR, Honig GR et al (1959) The uptake of a variety of amino acids into nuclear proteins of tumors and other tissues. Cancer Res 19:1030–1039

Christensen HN (1990) Role of amino acid transport and countertransport in nutrition and metabolism. Physiol Rev 70:43–76

Daemen BJ, Elsinga PH, Mooibroek J et al (1991) PET measurements of hyperthermia-induced suppression of protein synthesis in tumors in relation to effects on tumor growth. J Nucl Med 32:1587–1592

DeBoer JR, vander Laan BFAM, Oruim J et al (2002) Carbon-11 tyrosine PET for visualization and protein synthesis rate assessment of laryngeal and hypopharyngeal carcinomas. Eur J Nucl Med 29:1182–1187

Dimitrakopoulou-Strauss A, Strauss LG, Burger C (2001) Quantitative PET studies in pretreated melanoma patients: a comparison of 6-[^{18}F]fluoro-L-DOPA with ^{18}F-FDG and ^{15}O-water using compartment and noncompartment analysis. J Nucl Med 42:248–256

Duhaylongsod FG, Lowe VJ, Patz EF Jr, Vaughn AL, Coleman RE, Wolfe WG (1995) Lung tumor growth correlates with glucose metabolism measured by fluoride-18 fluorodeoxyglucose positron emission tomography. Ann Thorac Surg 60:1348–1352

Dunzendorfer U, Schmall B, Bigler RE et al (1981) Synthesis and body distribution of alpha-aminoisobutyric acid-L-^{11}C in normal and prostate cancer bearing rat after chemotherapy. Eur J Nucl Med 6:535–538

Dwamena BA, Sonnad SS, Angobaldo JO, Wahl RL (1999) Metastases from non-small cell lung cancer: mediastinal staging in the 1990s – meta-analytic comparison of PET and CT. Radiology 213:530–536

Erler JT, Cawthorne CJ, Williams KJ et al (2004) Hypoxia-mediated downregulation of Bid and Bax in tumors occurs via hypoxia inducible factor 1-dependent and -independent mechanisms and contributes to drug resistance. Mol Cell Biol 24:2875–2889

Flier JS, Mueckler MM, Usher P, Lodish HF (1987) Elevated levels of glucose transport and transporter messenger RNA are induced by ras or src oncogenes. Science 235:1492–1495

Graeber TG, Osmanian C, Jacks T et al (1996) Hypoxia-mediated selection of cells with diminished apoptotic potential in solid tumors. Nature 379:88–91

Grönroos T, Bentzen L, Marjamäki P, Murata R, Horsman MR, Keiding S, Eskola O, Haaparanta M, Minn H, Solin O (2004) Comparison of the biodistribution of two hypoxia markers [^{18}F]FETNIM and [^{18}F]FMISO in an experimental mammary carcinoma. Eur J Nucl Med Mol Imaging 31:513–520

Haberkorn U, Eisenhut M (2005) Molecular imaging and therapy – a programme based on the development of new biomolecules. Eur J Nucl Med Mol Imaging 32:1354–1359

Haberkorn U, Strauss LG, Dimitrakopoulou A, Engenhart R, Oberdorfer F, Ostertag H, Romahn J, van Kaick G (1991) PET studies of fluorodeoxyglucose metabolism in patients with recurrent colorectal tumors receiving radiotherapy. J Nucl Med 32:1485–1490

Haberkorn U, Reinhardt M, Strauss LG, Oberdorfer F, Berger MR, Altmann A, Wallich R, Dimitrakopoulou A, van Kaick G (1992) Metabolic design of combination therapy: use of enhanced fluorodeoxyglucose uptake caused by chemotherapy. J Nucl Med 33:1981–1987

Haberkorn U, Strauss LG, Dimitrakopoulou A et al (1993) Fluorodeoxyglucose imaging of advanced head and neck cancer after chemotherapy. J Nucl Med 34:12–17

Haberkorn U, Ziegler SI, Oberdorfer F, Trojan H et al (1994) FDG uptake, tumor proliferation and expression of glycolysis associated genes in animal tumor models. Nucl Med Biol 21:827–834

Haberkorn U, Altmann A, Morr I et al (1997a) Multi tracer studies during gene therapy of hepatoma cells with HSV thymidine kinase and ganciclovir. J Nucl Med 38:1048–1054

Haberkorn U, Bellemann ME, Altmann A, Gerlach L, Morr I, Oberdorfer F, Brix G, Doll J, Blatter J, Kaick G van (1997b) PET 2-fluoro-2-deoxyglucose uptake in rat prostate adenocarcinoma during chemotherapy with gemcitabine. J Nucl Med 38:1215–1221

Haberkorn U, Bellemann ME, Gerlach L, Morr I, Trojan H, Brix G, Altmann A, Doll J, van Kaick G (1998) Uncoupling of 2-fluoro-2-deoxyglucose transport and phosphorylation in rat hepatoma during gene therapy with HSV thymidine kinase. Gene Ther 5:880–887

Haberkorn U, Altmann A, Kamencic H, Morr I, Traut U, Henze M, Jiang S, Metz J, Kinscherf R (2001a) Glucose transport and apoptosis after gene therapy with HSV thymidine kinase. Eur J Nucl Med 28:1690–1696

Haberkorn U, Bellemann ME, Brix G, Kamencic H, Morr I, Traut U, Altmann A, Doll J, Blatter J, Kinscherf R (2001b) Apoptosis and changes in glucose transport early after treatment of Morris hepatoma with gemcitabine. Eur J Nucl Med 28:418–425

Haberkorn U, Kinscherf R, Krammer PH, Mier W, Eisenhut M (2001c) Investigation of a potential scintigraphic marker of apoptosis: radioiodinated Z-Val-Ala-DL-Asp(O-Methyl)-fluoromethyl ketone. Nucl Med Biol 28: 793–798

Haberkorn U, Altmann A, Eisenhut M (2002) Functional genomics and proteomics – the role of nuclear medicine. Eur J Nuc Med 29:115–132

Haberkorn U, Mier W, Eisenhut M (2005) Scintigraphic imaging of gene expression and gene transfer. Curr Med Chem 12:779–794

Haddad JJ (2002) Oxygen-sensing mechanisms and the regulation of redox-responsive transcription factors in development and pathophysiology. Respir Res 3:26

Hayes N, Biswas C, Strout HV, Berger J (1993) Activation by protein synthesis inhibitors of glucose transport into L6 muscle cells. Biochem Biophys Res Commun 190:881–887

Heesters MA, Go KG, Kamman RL et al (1998) ^{11}C-tyrosine positron emission tomography and ^{1}H magnetic resonance spectroscopy of the response of brain gliomas to radiotherapy. Neuroradiology 40:103–108

Heiss P, Mayer S, Herz M et al (1999) Investigation of transport mechanism and uptake kinetics of O-(2-[^{18}F]fluoroethyl)-L-tyrosine in vitro and in vivo. J Nucl Med 40:1367–1373

Herholz K, Holzer T, Bauer B et al (1998) ^{11}C-methionine PET for differential diagnosis of low-grade gliomas. Neurology 50:1316–1322

Hewitson KS, McNeill LA, Riordan MV et al (2002) Hypoxia-inducible factor (HIF) asparagine hydroxylase is identical to factor inhibiting HIF (FIH) and is related to the cupin structural family. J Biol Chem 277:26351–26355

Higashi K, Clavo AC, Wahl RL (1993) In vitro assessment of 2-fluoro-2-deoxy-D-glucose, L-methionine and thymidine as agents to monitor the early response of a human adenocarcinoma cell line to radiotherapy. J Nucl Med 34:773–779

Higashi K, Ueda Y, Yagishita M et al (2000) FDG PET measurement of the proliferative potential of non-small cell lung cancer. J Nucl Med 41:85–92

Hughes CS, Shen JW, Subjeck JR (1989) Resistance to etoposide induced by three glucose-regulated stresses in Chinese hamster ovary cells. Cancer Res 49:4452–4454

Inoue T, Shibasaki T, Oriuchi N et al (1999) ^{18}F alpha-methyl tyrosine PET studies in patients with brain tumors. J Nucl Med 40:399–405

Ishiwata K, Hatazawa J, Kubota K et al (1989) Metabolic fate of L-[methyl-^{11}C]methionine in human plasma. Eur J Nucl Med 15:665–669

Ishiwata K, Kubota K, Kubota R et al (1991) Selective 2-[^{18}F]fluorodopa uptake for melanogenesis in murine metastatic melanoma. J Nucl Med 32:95–101

Ishiwata K, Hatazawa J, Kubota K et al (1996) A feasibility study on L-[1-carbon11]tyrosine and L-[methyl-carbon-11]methionine to assess liver protein synthesis. J Nucl Med 37:279–285

Isselbacher KJ (1972) Sugar and amino acid transport by cells in culture: differences between normal and malignant cells. N Engl J Med 286:929–933

Jager PL, Plaat BE, deVries EG et al (2000) Imaging of soft tissue tumors using L-3-[iodine-123]iodo-alpha-methyl-tyrosine SPECT: comparison with proliferative and mitotic activity, cellularity and vascularity. Clin Cancer Res 6:2252–2259

Jager PL, Vaalburg W, Pruim J et al (2001) Radiolabeled amino acids: basic aspects and clinical applications in oncology. J Nucl Med 42:432–445

Jansson T, Westlin JE, Ahlstrom H et al (1995) Positron emission tomography studies in patients with locally advanced and/or metastatic breast cancer: a method for early therapy evaluation. J Clin Oncol 13:1470–1477

Kaschten B, Stevenaert A, Sadzot B et al (1998) Preoperative evaluation of 54 gliomas by PET with fluorine-18-fluorodeoxyglucose and/or carbon-11-methionine. J Nucl Med 39:778–785

Kubota K, Matsuzawa T, Fujiwara T et al (1989) Differential diagnosis of AH109A tumor and inflammation by radioscintigraphy with L-[methyl-^{11}C]-methionine. Jpn J Cancer Res 80:778–782

Kubota K, Matsuzawa T, Fujiwara T et al (1990) Differential diagnosis of lung tumor with positron emission tomography: a prospective study. J Nucl Med 31:1927–1932

Kuwert T, Probst-Cousin S, Woesler B et al (1997) Iodine-123-alpha-methyl tyrosine in glioma: correlation with cellular density and proliferative activity. J Nucl Med 38:1551–1555

Lando D, Peet DJ, Gorman JJ, Whelan DA, Whitelaw ML, Bruick RK (2002a) FIH-1 is an asparaginyl hydroxylase enzyme that regulates the transcriptional activity of hypoxia-inducible factor. Genes Dev 16:1466–1471

Lando D, Peet DJ, Whelan DA, Gorman JJ, Whitelaw ML (2002b) Asparagine hydroxylation of the HIF transactivation domain a hypoxic switch. Science 295:858–861

Langen KJ, Coenen HH, Roosen N et al (1990) SPECT studies of brain tumors with L-3-[^{123}I] iodo-alpha-methyl tyrosine: comparison with PET, ^{124}IMT and first clinical results. J Nucl Med 31:281–286

Langen KJ, Ziemons K, Kiwit JC et al (1997) 3-[^{123}I]iodo-alpha-methyltyrosine and [methyl-^{11}C]-L-methionine uptake in cerebral gliomas: a comparative study using SPECT and PET. J Nucl Med 38:517–522

Lee ST, Scott AM (2007) Hypoxia positron emission tomography imaging with ^{18}F-Fluoromisonidazole. Semin Nucl Med 37:451–461

Leskinen-Kallio S, Lindholm P, Lapela M et al (1994) Imaging of head and neck tumors with positron emission tomography and [^{11}C]methionine. Int J Radiat Oncol Biol Phys 30:1195–1199

Lindholm P, Leskinen S, Lapela M (1998) Carbon-11-methionine uptake in squamous cell head and neck cancer. J Nucl Med 39:1393–1397

Martin SJ, Reutelingsperger CPM, McGahon AJ (1995) Early redistribution of plasma membrane phosphatidylserine is a general feature of apoptosis regardless of the initiating stimulus: inhibition by overexpression of Bcl-2 and Abl. J Exp Med 182:1545–1556

McConathy J, Martarello L, Malveaux EJ et al (2002) Radiolabeled amino acids for tumor imaging with PET: radiosynthesis and biological evaluation of 2-amino-3-[^{18}F]fluoro-2-methylpropanoic acid and 3-[^{18}F]fluoro-2-methyl-2-(methylamino)propanoic acid. J Med Chem 45:2240–2249

Mosskin M, Bergstrom M, Collins VP et al (1986) Positron emission tomography with 11C-methionine of intracranial tumors compared with histology of multiple biopsies. Acta Radiol 369 Suppl:157–160

Ogawa T, Kanno I, Shishido F et al (1991) Clinical value of PET with ^{18}F-fluorodeoxyglucose and L-methyl-^{11}C-methionine for diagnosis of recurrent brain tumor and radiation injury. Acta Radiol 32:197–202

Ogawa T, Shishido F, Kanno I et al (1993) Cerebral glioma: evaluation with methionine PET. Radiology 186:45–53

Padhani AR, Krohn KA, Lewis JS, Alber M (2007) Imaging oxygenation of human tumors. Eur Radiol 17:861–872

Plaat B, Kole A, Mastik M et al (1999) Protein synthesis rate measured with L-[1-^{11}C]tyrosine positron emission tomography correlated with mitotic activity and MIB-1 antibody-detected proliferation in human soft tissue sarcomas. Eur J Nucl Med 26:328–332

Plate KH, Breier G, Weich HA, Risau W (1992) Vascular endothelial growth factor is a potential tumor angiogenesis factor in human gliomas in vivo. Nature 359:845–848

Rau FC, Weber WA, Wester HJ et al (2002) O-(2-[^{18}F]fluoroethyl)-L-tyrosine (FET): a tracer for differentiation of tumor from inflammation in murine lymph nodes. Eur J Nucl Med 29:1039–1046

Reske SN, Kotzerke J (2001) FDG-PET for clinical use results of the 3rd German Interdisciplinary Consensus Conference, "Onko-PET III", 21 July and 19 September 2000. Eur J Nucl Med 28:1707–1723

Rodriguez M, Rehn S, Ahstrom H et al (1995) Predicting malignancy grade with PET in non-Hodgkin's lymphoma. J Nucl Med 36:1790–1796

Rozental JM, Levine RL, Nickles RJ, Dobkin JA (1989) Glucose uptake by gliomas after treatment. A positron emission tomographic study. Arch Neurol 46:1302–1307

Saier MH, Daniels JR, Boerner P, Lin J (1988) Animal amino acid transport systems in animal cells: potential targets of oncogene action and regulators of cellular growth. J Membr Biol 104:1–20

Scanlon K, Safirstein RL, Thies H et al (1983) Inhibition of amino acid transport by cis-diaminedichloroplatinum (II) derivatives L1210 murine leukemia cells. Cancer Res 43:4211–4215

Scanlon K, Cashmore AR, Kashani-Sabet M et al (1987) Inhibition of methionine uptake by methotrexate in mouse leukemia L1210. Cancer Chemother Pharmacol 19:21–24

Schaider H, Haberkorn U, Berger MR et al (1996) Application of alpha-amino-isobutyric acid, L-methionine, thymidine and 2-fluoro-2-deoxy-D-glucose to monitor effects of chemotherapy in a human colon carcinoma cell line. Eur J Nucl Med 23:55–60

Schwarzbach M, Willeke F, Dimitrakopoulou-Strauss A et al (1999) Functional imaging and detection of local recurrence in soft tissue sarcomas by positron emission tomography. Anticancer Res 19:1343–1349

Semenza GL (2002) HIF-1 and tumor progression: pathophysiology and therapeutics. Trends Mol Med 8:S62–S67

Shawver LK, Olson SA, White MK, Weber MJ (1987) Degradation and biosynthesis of the glucose transporter protein in chicken embryo fibroblasts transformed by the src oncogene. Mol Cell Biol 7:2112–2118

Shoup TM, Olson J, Hoffman JM et al (1999) Synthesis and evaluation of [^{18}F]1-amino-3-fluorocyclobutane-1-carboxylic acid to image brain tumors. J Nucl Med 40:331–338

Sieger S, Jiang S, Schönsiegel F, Eskerski H, Kübler W, Altmann A, Haberkorn U (2003) Tumor-specific activation of the sodium/iodide symporter gene under control of the glucose transporter gene 1 promoter (GTI-1.3). Eur J Nucl Med Mol Imaging 30:748–756

Sieger S, Jiang S, Kleinschmidt J, Eskerski H, Schönsiegel F, Altmann A, Mier W, Haberkorn U (2004) Tumor-specific gene expression using regulatory elements of the glucose transporter isoform 1 gene. Cancer Gene Ther 11:41–51

Singh D, Banerji AK, Dwarakanath BS, Tripathi RP, Gupta JP, Mathew TL, Ravindranath T, Jain V (2005) Optimizing cancer radiotherapy with 2-deoxy-d-glucose dose escalation studies in patients with glioblastoma multiforme. Strahlenther Onkol 181:507–514

Stadler P, Becker A, Feldmann HJ et al (1999) Influence of the hypoxic subvolume on the survival of patients with head and neck cancer. Int J Radiat Oncol Biol Phys 44:749–754

Teicher BA (2004) Hypoxia and drug resistance. Cancer Metastasis Rev 13:139–168

Uehara H, Miyagawa T, Tjuvajev J et al (1997) Imaging experimental brain tumors with 1-aminocyclopentane carboxylic acid and alpha-aminoisobutyric acid: comparison to fluorodeoxyglucose and diethylenetriaminepentaacetic acid in morphologically defined tumor regions. J Cereb Blood Flow Metab 17:1239–1253

Vaalburg W, Coenen HH, Crouzel C et al (1992) Amino acids for the measurement of protein synthesis in vivo by PET. Int J Rad Appl Instrum B 19:227–237

Vansteenkiste JF, Stroobants SG, Dupont PJ et al (1999) Prognostic importance of the standardized uptake value on (18)F-fluoro-2-deoxy-glucose-positron emission tomography scan in non-small-cell lung cancer: an analysis of 125 cases. Leuven Lung Cancer Group. J Clin Oncol 17:3201–3206

Villa P, Kaufmann SH, Earnshaw WC (1997) Caspases and caspase inhibitors. Trends Biochem Sci 22:388–393

Weber WA, Wester HJ, Herz M et al (2001) Kinetics of F-18-fluoroethyl-L-tyrosine (FET) in patients with brain tumors. J Nucl Med 42:214P–215P

Wertheimer E, Sasson S, Cerasi E, Ben-Neriah Y (1991) The ubiquitous glucose transporter GLUT-1 belongs to the glucose-regulated protein family of stress-inducible proteins. Proc Natl Acad Sci U S A 88:2525–2529

Wester HJ, Herz M, Weber W et al (1999) Synthesis and radiopharmacology of O-(2-[^{18}F]fluoroethyl)-L-tyrosine for tumor imaging. J Nucl Med 40:205–212

Widnell CC, Baldwin SA, Davies A, Martin S, Pasternak CA (1990) Cellular stress induces a redistribution of the glucose transporter. FASEB J 4:1634–1637

Wienhard K, Herholz K, Coenen HH et al (1991) Increased amino acid transport into brain tumors measured by PET of L-(2-^{18}F)fluorotyrosine. J Nucl Med 32:1338–1346

Willemsen AT, vanWaarde A, Paans AM et al (1995) In vivo protein synthesis rate determination in primary or recurrent brain tumors using L-[1-^{11}C]-tyrosine and PET. J Nucl Med 36:411–419

Wurker M, Herholz K, Voges J et al (1996) Glucose consumption and methionine uptake in low-grade gliomas after iodine-125 brachytherapy. Eur J Nucl Med 23:583–586

Young SD, Marshall RS, Hill RP (1988) Hypoxia induces DNA overreplication and enhances metastatic potential of murine tumor cells. Proc Natl Acad Sci U S A 85:9533–9537

Zwaal RFA, Schroit AJ (1997) Pathophysiologic implications of membrane phospholipid asymmetry in blood cells. Blood 89:1121–1132